

## **A TOTAL-CONCENTRATION FIXED-GRID METHOD FOR TWO-DIMENSIONAL DIFFUSION-CONTROLLED WET CHEMICAL ETCHING**

**P. Rath,<sup>1</sup> J. C. Chai,<sup>1\*</sup> H. Y. Zheng,<sup>2</sup> Y. C. Lam,<sup>1</sup> V. M. Murukeshan<sup>1</sup>**

<sup>1</sup>School of Mechanical and Aerospace Engineering, Nanyang Technological University, Singapore 639798

<sup>2</sup>Singapore Institute of Manufacturing Technology, Singapore 638075

\*mckchai@ntu.edu.sg

### **ABSTRACT**

This article presents a total concentration method for two-dimensional wet chemical etching. The proposed procedure is a fixed-grid approach. It is analogous to the enthalpy method used for modeling melting/solidification problems. The governing equation is formulated using the total concentration of the etchant. It includes the reacted and the unreacted concentrations of the etchant. The proposed governing equation includes the interface condition. The reacted concentration is used to capture the etchant-substrate interface implicitly. Since the grids are fixed, a diffusion problem remains a diffusion problem unlike the moving grid approach where the diffusion problem becomes the convection-diffusion problem due to the mesh velocity. For demonstration purposes, the finite volume method is used to solve for the transient concentration distribution of etchant. In this article, two-dimensional diffusion-controlled wet chemical etching processes are modeled. The results obtained from the proposed total concentration method are compared with available "analytic" solutions and solutions from moving-grid approach.

### **INTRODUCTION**

Wet chemical etching (WCE) is a process by which materials selectively removed from the surface of a substrate to form a specific pattern on the substrate surface. This is achieved by the reaction of liquid etchant in contact with the substrate. WCE process widely used in the manufacturing of shadow mask for color-television tubes [1], IC devices in microelectronics industries [2], MEMS devices such as hinges [3] and pressure sensors [4] etc.

Various mathematical models have been proposed by different researchers to model the WCE process in order to predict the etched pattern structure on the substrate surface during the progress of etching. Those models are the asymptotic solution [5, 6], the variational inequality approach [7, 8], the moving-grid (MG) approach [7, 10-12], the level-set method [13, 14], and the fixed-grid (FG) method [15, 16].

Based on the rate of reaction, two possible cases of WCE process can exist namely- the diffusion-controlled [5-10, 15, 16] and the reaction-controlled [7, 10-12, 14, 16] etching. These two cases are studied in the modeling of one-dimensional [9, 11, 15, 16] and two-dimensional [5-10, 12-14] WCE using the above analytical and numerical approaches.

The analytical solution to two-dimensional WCE is presented by Kuiken [5, 6] using asymptotic solution. The asymptotic solution is valid for diffusion-controlled etching using a dilute etchant. Kuiken et al. [9] also presented the exact solution for the diffusion-controlled WCE in a one-dimensional geometry. The analytical treatment is then extended to a two-dimensional diffusion-controlled WCE based on the perturbation principle.

The MG method is the widely used numerical method to model WCE process. In the MG method, since the computational domain is limited to the space occupied by the etchant, it continuously expands with time. As the computational domain expands with time, the computation mesh has to be regenerated at every time step. Due to the movement of the mesh, a diffusion problem becomes a convection-diffusion problem. The mesh velocities are accounted for in the governing equation in terms of an extra convective term [7, 12]. Further, an unstructured mesh system or a body-fitted grid system is needed to model multidimensional WCE.

Chai and co-workers [15, 16] presented a fixed-grid approach based on the total concentration of etchant to model WCE process. This method is analogous to the enthalpy method used in the modeling of melting/solidification process [17, 18]. The total concentration is the sum of the unreacted etchant concentration and the reacted etchant concentration. The governing equation based on the total concentration includes the interface condition. In this formulation, the reacted concentration of the etchant is a measure of the etchfront profile during the etching process. Unlike the MG method, the etchfront is found implicitly with the total concentration

method. Since the grids are fixed, there is no grid velocity. Hence a diffusion problem always remains a diffusion problem. Cartesian grid can be used to capture the complicated etchfront evolution in multidimensional etching. The model has been tested for one-dimensional diffusion-controlled [15] and reaction-controlled [16] WCE.

In this article, the fixed-grid (FG) method is extended to model two-dimensional diffusion-controlled WCE. A two-dimensional WCE problem, the governing equation, the interface condition and the boundary conditions are described. Various ingredients of the proposed FG method are then discussed. The overall solution procedure is then summarized. A brief description of the numerical method used in this article is given. Discussions of the results obtained using the proposed FG method are presented. Some concluding remarks are then given to conclude this article.

## NOMENCLATURE

$a$	coefficient of the discretization equation
$c$	unreacted etchant concentration
$c_R$	reacted etchant concentration
$c_{R,max}$	maximum possible value of the reacted concentration
$c_T$	total concentration
$D$	diffusion coefficient of etchant
$M_{Sub}$	molecular weight of the substrate
$m$	stoichiometric reaction parameter
$t$	time
$t^*$	non-dimensional time
$v_{\bar{n}}$	normal velocity of the etchant-substrate interface
$x, y$	coordinate directions
$X, Y$	non-dimensional coordinate directions

## Greek Symbols

$\alpha$	underrelaxation factor
$\nabla$	vector differential operator
$\Delta t$	time step
$\rho_{Sub}$	density of the substrate
$\beta$	non-dimensional etching parameter

## Subscripts

$o$	initial
$P$	control volume P
$Sub$	the substrate
$Et$	the etchant
$T$	total

## Superbscripts

$m$	iteration number
$o$	previous time step

## PROBLEM DESCRIPTION AND GOVERNING EQUATIONS

The schematic and computational domain for the two-dimensional problem considered is shown in Figs. 1. A gap of width  $2a$  is to be etched in a cavity as shown in Fig. 1a. The initial concentration of the etchant at  $t = 0$  is  $c_o$ . At  $t > 0$ , the

reaction between the etchant and the substrate at the etchant-substrate interface results in the reduction of the concentration of etchant adjacent to the etchant-substrate interface and the depletion of the substrate. The concentration of etchant on the boundaries far away from the gap is kept at the initial concentration, i.e.  $c = c_o$ . The etching is assumed diffusion-controlled where reaction rate is infinitely fast. The origin of the coordinate system is set to the etchant-substrate interface at the center of the gap. Since the problem is symmetrical about the origin in Fig. 1, only half of the domain is considered as shown in Fig. 1b. The governing equation, the initial condition, the interface condition and the boundary conditions are presented next.

For a stationary etchant solution, the etchant concentration within the etchant domain is governed by the mass diffusion equation given by

$$\frac{\partial c}{\partial t} = \frac{\partial}{\partial x} \left( D \frac{\partial c}{\partial x} \right) + \frac{\partial}{\partial y} \left( D \frac{\partial c}{\partial y} \right) \quad \text{in } \Omega(t), t > 0 \quad (1a)$$

The initial and boundary conditions are

$$c = c_o \quad \text{in } \Omega(t), t = 0 \quad (1b)$$

$$c = 0 \quad \text{on } f(t) \quad (1c)$$

Remaining boundary conditions are shown in Fig. 1b. The interface condition at the etchant-substrate interface is given as

$$\bar{v} = - \frac{DM_{Sub}}{m\rho_{Sub}} \nabla c \quad (1d)$$

where  $\bar{v}$  is the velocity of the etchant-substrate interface,  $D$  is the diffusion coefficient of etchant,  $M_{Sub}$  is the molecular weight of the substrate,  $\rho_{Sub}$  is the density of the substrate and  $m$  is the stoichiometric reaction parameter of the etchant-substrate reaction.

## THE TOTAL CONCENTRATION METHOD

In this article the total concentration of the etchant is defined as

$$c_T \equiv c + c_R \quad (2)$$

where  $c_T$  is the total concentration,  $c$  is the unreacted etchant concentration and  $c_R$  is the reacted etchant concentration respectively. Physically,  $c_R$  is the etchant concentration consumed in the reaction process. As such it is constant except at the etchant-substrate interface. This is used to capture the etchfront implicitly. The value of  $c_R$  changes from 0 to its maximum possible value of  $c_{R,max}$  in a control volume where etching is taking place. The maximum possible value of the reacted concentration termed  $c_{R,max}$ , is the amount of etchant required per unit volume of substrate to dissolve the substrate during reaction. It is given as

$$c_{R,max} = \frac{m\rho_{Sub}}{M_{Sub}} \quad (3)$$

The governing equation based on the total concentration is given by

$$\frac{\partial c_T}{\partial t} = \frac{\partial}{\partial x} \left( D \frac{\partial c}{\partial x} \right) + \frac{\partial}{\partial y} \left( D \frac{\partial c}{\partial y} \right) \quad (4)$$

Using Eq. (2), Eq. (4) can be written as

$$\frac{\partial c}{\partial t} = \frac{\partial}{\partial x} \left( D \frac{\partial c}{\partial x} \right) + \frac{\partial}{\partial y} \left( D \frac{\partial c}{\partial y} \right) - \frac{\partial c_R}{\partial t} \quad (5)$$

This equation is valid in both the etchant and the substrate regions. The interface condition given by Eq. (1d) is contained in Eq. (5) implicitly. A procedure to update the reacted concentration ( $c_R$ ) is needed to complete the formulation. This is discussed next.

### **PROCEDURE TO UPDATE $c_R$**

In the proposed FG method, the etching-control-volumes (ECV) are first identified as shown in Fig. 2. The ECVs are the substrate control volumes adjacent to the etchant control volumes where reaction between etchant and substrate is taking place. In an ECV,  $c_R$  changes from 0 to its maximum possible value of  $c_{R,max}$ . The finite volume discretization equation (using the fully implicit scheme) of Eq. (5) for an ECV (control volume P) is given as

$$a_P c_P^m = \sum a_{nb} c_{nb}^m + a_P^o c_P^o - (c_{R,P}^m - c_{R,P}^o) \frac{\Delta V_P}{\Delta t} \quad (6)$$

where  $m$  is the  $m^{\text{th}}$  iteration of the current time step,  $o$  is the previous time step,  $P$  is the control volume  $P$ ,  $nb$  is the neighboring control volumes,  $a$  is the coefficients of the discretization equation,  $\Delta V$  is the volume of a control volume and  $\Delta t$  is the time step respectively. It is to be noted that Eq (6) is valid for all control volumes. Since,  $c_R$  is constant in the etchant and substrate regions, the last term on the right side of Eq. (6) is zero except in the ECV. At the  $(m+1)^{\text{th}}$  iteration, Eq. (6) can be written as

$$a_P c_P^{m+1} = \sum a_{nb} c_{nb}^{m+1} + a_P^o c_P^o - (c_{R,P}^{m+1} - c_{R,P}^o) \frac{\Delta V_P}{\Delta t} \quad (7)$$

Subtracting Eq. (7) from Eq. (6) and rearranging, gives

$$c_{R,P}^{m+1} = c_{R,P}^m + \frac{\Delta t}{\Delta V_P} \left[ a_P (c_P^m - c_P^{m+1}) + \sum a_{nb} (c_{nb}^{m+1} - c_{nb}^m) \right] \quad (8)$$

When the solution converges, the last term of Eq. (8) will be zero. However, during the initial iteration process, it is most likely a non-zero term. Realizing that it is zero upon convergence, this term can be ignored from the calculation and Eq. (8) becomes

$$c_{R,P}^{m+1} = c_{R,P}^m + \alpha a_P \frac{\Delta t}{\Delta V_P} (c_P^m - c_P^{m+1}) \quad (9)$$

where  $\alpha$  is an under-relaxation factor. For a diffusion-controlled reaction, the reaction rate at the interface is infinitely fast which makes the concentration at the interface zero. For diffusion-controlled reaction, FG procedure ensures that  $c_P^{m+1} = 0$  and the excess concentration is used to update the reacted concentration. With  $c_P^{m+1} = 0$ , Eq. (9) becomes

$$c_{R,P}^{m+1} = c_{R,P}^m + \alpha a_P \frac{\Delta t}{\Delta V_P} c_P^m \quad (10)$$

In the ECVs, the reacted concentration is updated using Eq. (10). Etching for a given ECV completed, when  $c_{R,P}^{m+1}$  reaches  $c_{R,max}$ .

### **OVERALL SOLUTION PROCEDURE**

The overall solution procedure for the proposed total concentration method can be summarized as follows:

1. Specify the etchant domain, the substrate domain and the mask region. Ensure that the etchant-substrate interface lies on the interface between two control volumes.
2. Set the initial etchant concentration as  $c_o$  in the etchant domain and zero in the substrate domain including the mask region.
3. Initially set  $c_R$  to 0 in the substrate domain including the mask region and to  $c_{R,max}$  in the etchant domain respectively.
4. Advance the time step to  $t + \Delta t$ .
5. Identify the etching control volumes (ECVs).
6. Use the ‘‘internal’’ boundary condition treatment of Patankar [19] (by setting  $S_P$  to a big number) to set the unreacted etchant concentration in the mask and substrate regions to zero.
7. Set  $S_P$  in the ECV to zero.
8. Solve Eq. (5) for the unreacted concentration.
9. Update the reacted concentration in the ECVs using Eq. (10).
10. Check for convergence.
  - a) If the solution has converged, then check if the required number of time steps has been reached. If yes, stop. If not, repeat (4) to (9).

- b) If the solution has not converged, then check the calculated reacted concentration.

- If  $c_R < c_{R,max}$ , repeat (8) to (9).
- If  $c_R \geq c_{R,max}$ , then set  $c_R = c_{R,max}$  and repeat (5) to (9).

## NUMERICAL METHOD

In this article, the finite-volume method (FVM) of Patankar [19] is used to solve the diffusion equation (Eq. 5). Since a detailed discussion of the FVM is available in Patankar [19], only a brief description of the major features of the FVM used is given here. In the FVM, the domain is divided into a number of control volumes such that there is one control volume surrounding each grid point. The grid point is located in the center of a control volume. The governing equation is integrated over each control volume to derive an algebraic equation containing the grid point values of the dependent variable. The discretization equation then expresses the conservation principle for a finite control volume just as the partial differential equation expresses it for an infinitesimal control volume. The resulting solution implies that the integral conservation of mass is exactly satisfied for any control volume and of course, for the whole domain. The resulting algebraic equations are solved using a line-by-line Tri-Diagonal Matrix Algorithm. In the present study, a solution is deemed converged when the maximum change in the concentration and the maximum change in the reacted concentration between two successive iterations are less than  $10^{-11}$ .

## RESULTS AND DISCUSSIONS

The two-dimensional problem shown in Fig. 1 is modeled using the proposed total concentration approach. Due to the symmetry of the problem about the y-axis, only half of the domain is modeled as shown in Fig. 1b. For ease of presentation, the following dimensionless variables are defined.

$$X = x/a \quad (11a)$$

$$Y = y/a \quad (11b)$$

$$C = c/c_o \quad (11c)$$

$$C_R = c_R/c_o \quad (11d)$$

$$t^* = tD/a^2 \quad (11e)$$

$$\beta = \frac{m\rho_{Sub}}{c_o M_{Sub}} \quad (11f)$$

The non-dimensional width of the mask is taken as  $L_1 = l_1/a = 6.5$  and the dimensionless height of etchant is taken as  $L_3 = l_3/a = 6.5$ . The width and thickness of the substrate are taken as  $L_{Sub} = 1 + L_1 = 7.5$  and  $L_2 = l_2/a = 4.0$  respectively. Results for two mask thicknesses namely, infinitely thin and finite thickness are modeled. For infinitely thin mask, the non-dimensional mask thickness is taken as  $H = h/a = 0.005$ . Further decrease in mask thickness does not alter the solution.

For finite mask thickness, the thickness of the mask is taken as one-fourth of the gap width, i.e.  $H = h/a = 0.5$ .

A grid refinement study was performed to ensure the solutions are grid (temporal and spatial) independent. Figure 3 shows the evolution of etch profiles at four different times for  $\beta = 100$  and infinitely thin mask. Three control volume sizes are taken to carry out this test. For each control volume size the time independent etch profiles are shown. For the grid sizes of  $32 \times 29$  and  $72 \times 53$ , the time step size is  $\Delta t^* = 0.01$ . For the  $144 \times 104$  grid, the time step size is  $\Delta t^* = 0.001$ . It is seen that the grid sizes of  $72 \times 53$  and  $144 \times 104$  produced the same etch profile for the four given times. As a result,  $72 \times 53$  control volumes with  $\Delta t^* = 0.01$  are used in this article.

Figure 4 shows the comparisons of etch profiles at different times between the FG method, the asymptotic solution [6] and the MG [10] method. The non-dimensional etching parameter is taken as  $\beta = 100$ . It is seen from Fig. 4 that the present approach predicts the etch profiles at different times accurately. Some bulging effect is seen near the corner of the mask. The etching is faster near the corner region compared to the region away from the corner. Figure 5 shows the concentration contours at  $t^* = 30$ . It is seen that the concentration contours have gone deep into the etched region near the corner of the mask. Hence, the concentration gradient is higher near the mask region. As a result the etching is faster in this region which results in bulging of etch profiles. Figure 6 shows the comparison of etch profiles for  $\beta = 10$ . The etch profiles from the present approach compare very well with the variational inequality approach of Bruch et. al. [8]. The bulging region is enlarged from mask corner to the center compared to the case with  $\beta = 100$ . This is because of the high initial etchant concentration for  $\beta = 10$ , which results in faster etch rate. The bulging effect is localized near the mask corner region only at early time when  $\beta$  decreases to 10 from 100.

Figure 7 shows the comparisons of the etch profiles evolution for finite mask thickness. The non-dimensional etching parameter is taken as  $\beta = 100$ . The etch profiles obtained from the present approach compare well with the MG solutions [10]. Figure 8 shows the concentration contour at  $t^* = 126$ . It is seen that the concentration contours in the etched region is nearly flat. As a result, the concentration gradient will also be nearly uniform. Hence there is no significant bulging effect seen unlike the case with infinitely thin mask. Figure 9 shows the etch profiles obtained with both mask thicknesses. It is seen that the bulging effects reduces with mask thickness. It is because of the larger diffusion length of the etchant from the area above the inert mask to the etching surface. Hence fresh etchant is less readily available near the mask corner as thickness of the mask increases which results in slow etch rate near the mask corner.

## CONCLUDING REMARKS

A new fixed-grid method based on the total-concentration of etchant has been presented for two-dimensional WCE. The proposed method is analogous to the enthalpy method used in the modeling of melting/solidification

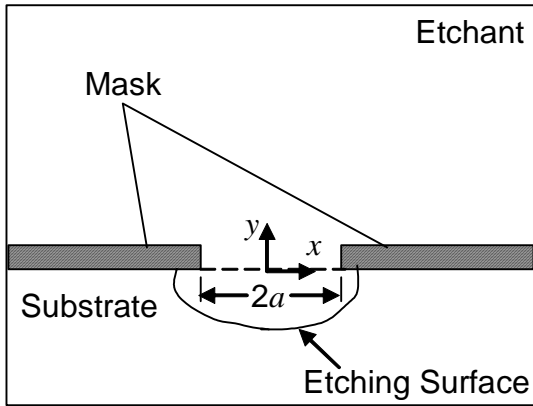
processes. A detailed formulation based on the total concentration of the etchant is presented. In the proposed approach the governing equation includes the interface condition. With this proposed method there is no necessity for computing the etchfront position explicitly. The method has been applied to two-dimensional diffusion-controlled etching. For demonstration purposes, the finite-volume method is used to discretize the governing equation. The results from the present approach are compared with the results from other existing methods. The results show that the etchfront profile can be predicted accurately using the proposed method.

## ACKNOWLEDGMENTS

This work was supported in part by SIMTech and Nanyang Technological University under SIMTech CRP, U03-S-097B.

## REFERENCES

- Hoffman K. H. and Sprekels J., 1990, Free boundary problems: theory and applications, *Longman Scientific and Technical* 1, pp. 89.
- Madou M. J., 2002, Fundamentals of microfabrication, 2<sup>nd</sup> Edition (CRC Press, New York).
- Pister K. S. J., Judy M. W., Burgett S. R. and Fearing R. S., 1992, Microfabricated hinges, *Sensors and Actuators A* **33**, pp. 249-256.
- Mastrangelo C. H., Zhang X. and Tang W. C., 1995, Surface micromachined capacitive differential pressure sensor with lithographically-defined silicon diaphragm, *The 8<sup>th</sup> International Conference on Solid-State Sensors and Actuators*, Eurosens IX (Stockholm June 25-29), pp. 612-615.
- Kuiken H. K., 1984, Etching: a two-dimensional mathematical approach, *Proceedings of the Royal Society of London A* **392**, pp. 199-225.
- Kuiken H. K., 1984, Etching through a slit, *Proceedings of the Royal Society of London A* **396**, pp. 95-117.
- Vuik C. and Cuvelier C., 1985, Numerical solution of an etching problem, *Journal of Computational Physics* **59**, pp. 247-263.
- Bruch J. C. Jr., Papadopoulos C. A. and Sloss J. M., 1993, Parallel computing used in solving wet chemical etching semiconductor fabrication problems, *GAKUTO International Series, Mathematical Sciences and Applications* **1**, pp. 281-292.
- Kuiken H. K., Kelly J. J. and Notten P. H. L., 1986, Etching profiles at resist edges - I. Mathematical models for diffusion-controlled cases, *Journal of the Electrochemical Society* **133**, pp. 1217-1226.
- Shin C. B. and Economou D. J., 1989, Effect of transport and reaction on the shape evolution of cavities during wet chemical etching, *Journal of the Electrochemical Society* **136**, pp. 1997-2004.
- Li W. J., Shih J. C., Mai J. D., Ho C-M., Liu J. and Tai Y-C., 1998, Numerical simulation for the sacrificial release of MEMS square diaphragms, *1st International Conference on MSMSSA* (San Jose, USA, April).
- Kaneko K., Noda T., Sakata M. and Uchiyama T., 2003, Observation and numerical simulation for wet chemical etching process of semiconductor, *Proceedings of 4<sup>th</sup> ASME-JSME Joint Fluids Engineering Conference* (Honolulu, USA, July 6-10).
- Adalsteinsson D. and Sethian J. A., 1995, A level set approach to a unified model for etching, deposition and lithography I: Algorithms and two-dimensional simulations, *Journal of Computational Physics* **120**, pp. 128-144.
- La Magna A., D'Arrigo G., Garozzo G. and Spinella C., 2003, Computational analysis of etched profile evolution for the derivation of 2D dopant density maps in silicon, *Materials Science and Engineering B* **102** (1-3), pp. 43-48.
- Lam Y. C., Chai J. C., Rath P., Zheng H. and Murukeshan V. M., 2004, A fixed grid method for chemical etching, *International Communications in Heat and Mass Transfer* **31** (8), pp. 1123-1131.
- Rath P., Chai J. C., Zheng H., Lam Y. C., Murukeshan V. M. and Zhu H., 2004, A fixed-grid approach for diffusion- and reaction-controlled wet chemical etching, *International Journal of Heat and Mass Transfer*, in press.
- Shamsundar N. and Sparrow E. M., 1975, Analysis of multidimensional conduction phase change via the enthalpy method, *Journal of Heat Transfer* **97**, pp. 333-340.
- Brent A. D., Voller V. R. and Reid K. J., 1988, Enthalpy-porosity technique for modeling convection-diffusion phase change: application to the melting of a pure metal, *Numerical Heat Transfer* **13**, pp. 297-318.
- Patankar S. V., 1980, *Numerical Heat Transfer and Fluid Flow, 1<sup>st</sup> edition* (Hemisphere, New York).



(a)

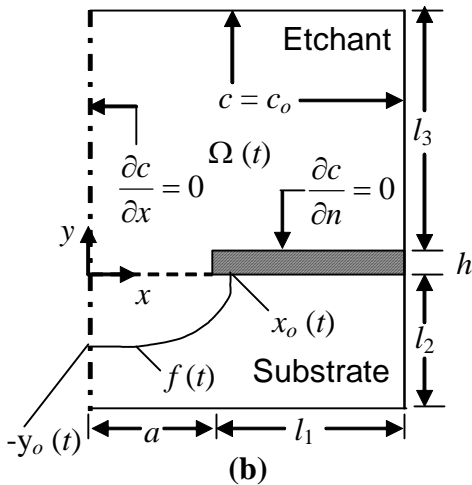


Figure 1. Schematic of the two-dimensional etching problem with finite gap width.

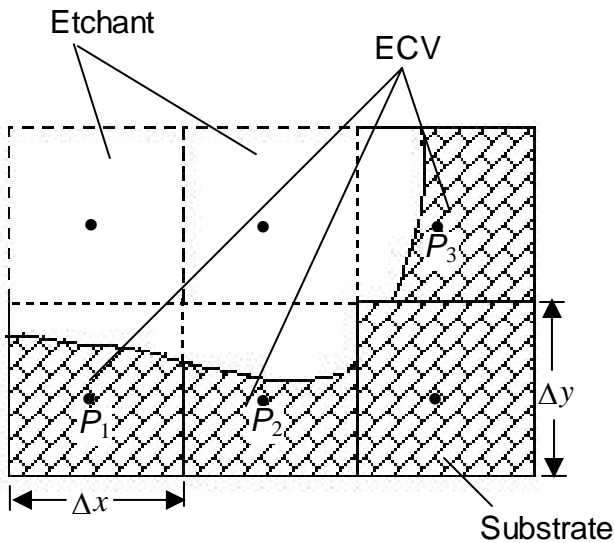


Figure 2. Control volumes P1, P2, P3 undergoing etching.

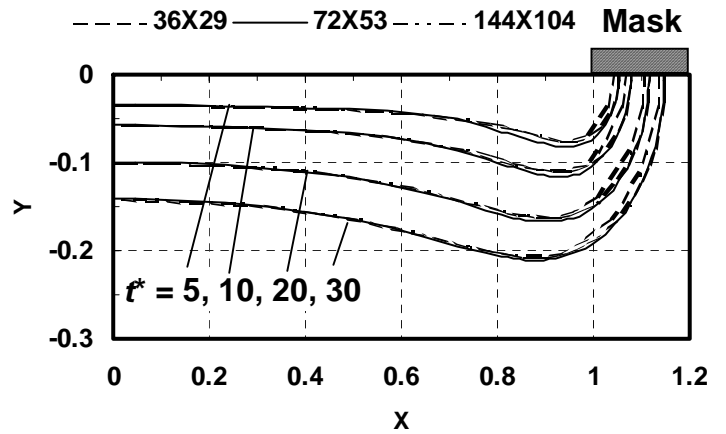


Figure 3. Grid independent study for  $\beta = 100$  and infinitely thin mask.

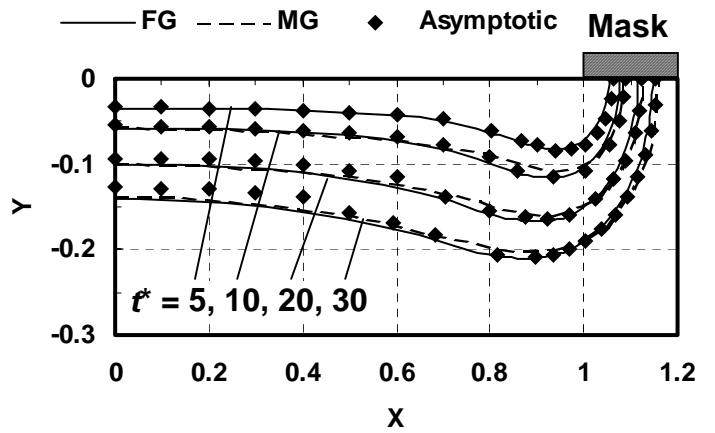


Figure 4. Comparison of etched profiles with existing asymptotic solution and MG method for  $\beta = 100$  and infinitely thin mask.

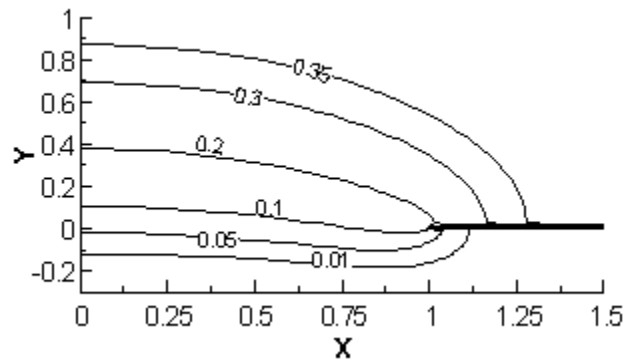


Figure 5. Concentration contours at  $t^* = 30$  for  $\beta = 100$  and infinitely thin mask.

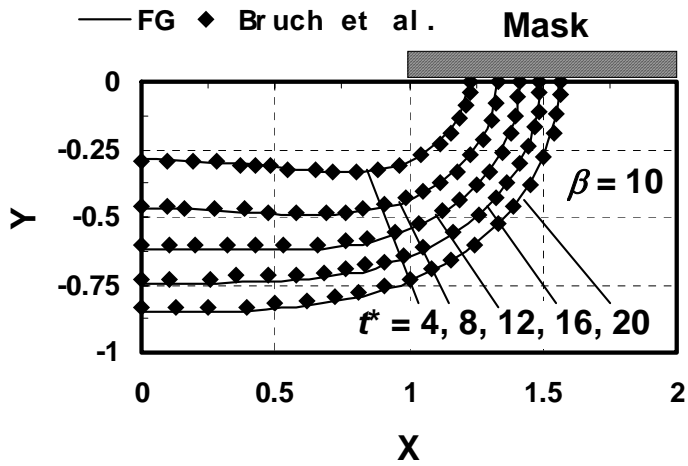


Figure 6. Comparison of etched profiles with the variational inequality approach for  $\beta = 10$  and infinitely thin mask.

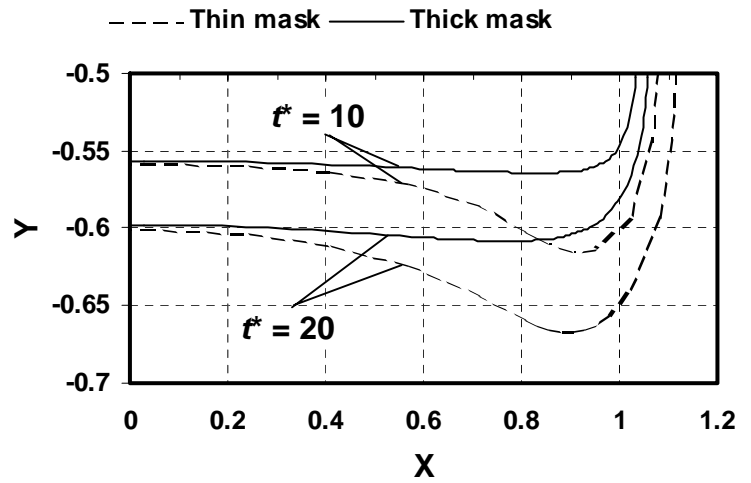


Figure 9. Effect of mask thickness on bulging of etched profile for  $\beta = 100$ .

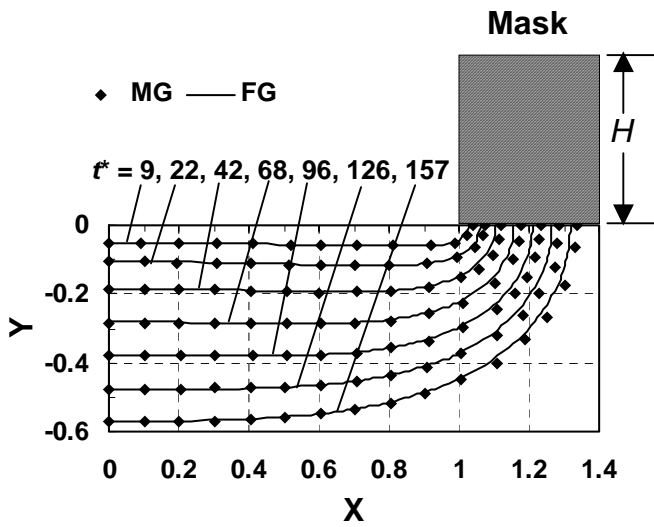


Figure 7. Comparison of etched profiles with MG method for  $\beta = 100$  and finite mask thickness ( $H = 0.5$ ).

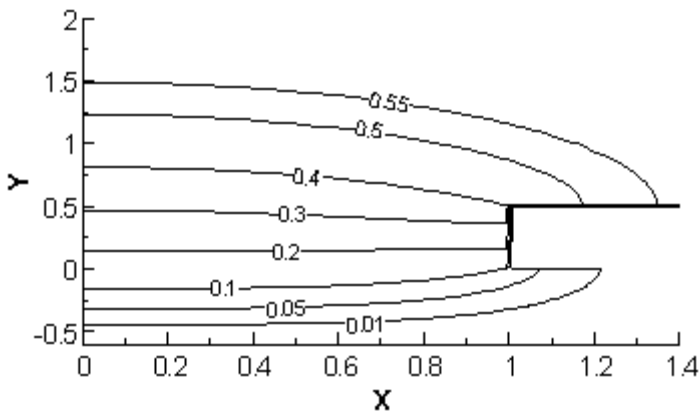


Figure 8. Concentration contour at  $t^* = 126$  for  $\beta = 100$  and finite mask thickness ( $H = 0.5$ ).